

Ultrafast Photoemission Spectroscopy of the Uranium Dioxide UO_2 Mott Insulator: Evidence for a Robust Energy Gap Structure

Steve M. Gilbertson,¹ Tomasz Durakiewicz,² Georgi L. Dakovski,³ Yinwan Li,² Jian-Xin Zhu,⁴ Steven D. Conradson,⁵ Stuart A. Trugman,⁴ and George Rodriguez^{1,*}

¹Center for Integrated Nanotechnologies, Los Alamos National Laboratory, MS K771, Los Alamos, New Mexico 87545, USA

²Condensed Matter and Magnet Science Group, Los Alamos National Laboratory, MS K764, Los Alamos, New Mexico 87545, USA

³SLAC National Accelerator Laboratory, 2575 Sand Hill Road, Menlo Park, California 94025, USA

⁴Physics of Condensed Matter and Complex Systems Group, Los Alamos National Laboratory, MS B262, Los Alamos, New Mexico 87545, USA

⁵Structure Property Relations Group, Los Alamos National Laboratory, MS G775, Los Alamos, New Mexico 87545, USA

(Received 3 April 2013; published 28 February 2014)

Time-resolved photoemission spectroscopy utilizing a probe energy of 32.55 eV and a pump energy of 3.1 and 4.65 eV with 30 fs temporal resolution is used to study the carrier dynamics in the 5*f* Mott insulator uranium dioxide (UO_2). The Mott gap and on-site Coulomb interaction energies are measured directly as $E_{\text{gap}} = 2.5$ eV and $U_C = 5$ eV, respectively, and the dynamics of the upper Hubbard band is mapped. The *f-f* Mott-Hubbard dynamics involves subpicosecond fluence-dependent relaxation, followed by decay via coupling to the lattice upon formation of excitonic polarons. Instead of an expected metallic transition, we observe a robust Mott gap structure, even at high pump fluences.

DOI: 10.1103/PhysRevLett.112.087402

PACS numbers: 78.66.Nk, 71.20.-b, 78.47.J-, 79.60.-i

Mott-Hubbard insulators belong to a class of strongly correlated systems that continue to attract broad interest. Their propensity to display unusual particle correlations stemming from short- and long-range interactions results in a plethora of novel and not fully understood phenomena such as nontrivial phase transitions, emergent behavior, orbital hybridization, and carrier thermalization [1–3]. The underexplored dynamical aspect is of growing interest, with some Mott-Hubbard systems expected to have extremely long-lived excited state carrier dynamics [4] because of inefficient coupling to various scattering channels. Because of the large Mott gap in strongly correlated complex oxides, there is also a growing practical interest in these systems as potential photovoltaic device candidates if quenching upon optical excitation into the upper band can be controlled to maintain charge separation [5].

Here we explore perhaps the least understood aspect of the ultrafast dynamics in the widely utilized Mott insulator UO_2 . At the forefront of ultrafast science in such systems have been studies on light-induced ultrafast insulator-metal phase transitions (IMT), where it was found that competing interactions between lattice structural Peierls-type distortions and/or dynamic charged population delocalizations may induce a Mott gap collapse [1–3,6]. It is also interesting from the perspective of large Coulomb interaction, as in vanadium dioxide (VO_2) and also uranium dioxide (UO_2), where site correlations determine the boundary between Mott-Hubbard and band insulator classification [7]. Knowing the value of the Coulomb on-site interaction U_C , which from the practical and modeling point of view is a measure of the energy difference between

the lower and upper Hubbard bands, is crucial in being able to model these systems by using the most recent theoretical approaches [8]. However, no direct measure of U_C is available. We propose that, by measuring directly the density of states by using time-resolved photoemission spectroscopy (TRPES) working in the pump-probe mode with fine-tuned characteristics like pump and probe photon energies, we can excite carriers across the Mott gap and establish the value of the gap and U_C directly. The ensuing ultrafast dynamics of quasiparticles in the upper Hubbard band is used to identify the dominating relaxation pathways.

At room temperature, UO_2 is a paramagnetic Mott-Hubbard-type insulator with a cubic fluorite crystal structure [Fig. 1(a)] [7]. Experiments and theory [7,9] determined a band gap of $E_{\text{gap}} = 2.3$ eV at room temperature. The density of states around the gap is characterized by localized 5*f* electronic character [7,10] with only a minute amount of hybridization, as evidenced by the extremely small 5*f* band dispersion of the order of 0.1 eV at a binding energy of 2 eV. Much more strongly hybridized and dispersive bands of mixed U(5*f*)-O(2*p*) orbital character are found at higher binding energies within the valence band [7]. Because of a sufficiently strong Coulomb interaction strength (U_C) indirectly established to be $U_C = 4.6$ eV, a Mott gap is formed between an occupied lower Hubbard band (LHB) and an unoccupied upper Hubbard band (UHB) [Fig. 1(b)]. This type of electronic structure raises unique questions about the dynamical behavior of electrons promoted across the Mott gap. The low-energy excitations across the gap are

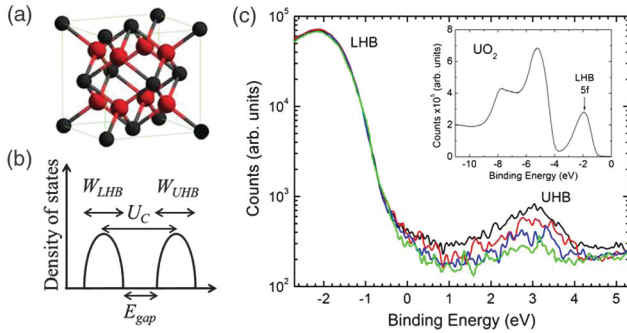


FIG. 1. (a) UO₂ fluorite crystal structure: U atoms are red, and O atoms are black. (b) Density of states band diagram for Mott-Hubbard insulator: W is the energy bandwidth, U_C is the Coulomb energy, and E_{gap} is the energy band gap. (c) Time-resolved PES study of the Mott insulator UO₂. Shown is the appearance of the UHB in the PES spectrum when pumping with 30-fs 4.65-eV pump photons at a fluence of $F = 0.51$ (black), 0.39 (red), 0.26 (blue), and 0.13 mJ/cm² (green), respectively. The trace data in the plot are at zero pump-probe time delay. The probe photon energy is 32.55 eV. The zero in the abscissa represents the position of the Fermi level E_F . The inset plot in (c) shows the PES spectrum for the static (no pump) case where the $5f$ electron dominated LHB is clearly identified. The peaks at binding energies less than -4 eV in the inset are associated with O $2p$ states [12].

of $5f$ - $5f$ character [9–12], forming doublons U^{3+} and holons U^{5+} among a “sea” of unexcited U^{4+} sites. The well-localized, narrow-bandwidth nature of the $5f$ electronic states suggests that these holon-doublon excitations may remain localized on f sites, causing restriction of the electron mobility to form a stable bosonic exciton predicted to have a long lifetime [4]. Further complexity arises from the presence of electronic defect states in imperfect crystals that give rise to phonon-assisted hopping (polaron conduction), leading to the formation of small polarons through the electron-longitudinal optical phonon interaction [9]. Finally, upon sufficiently strong photoexcitation typically in the mJ/cm² range, the rise in electronic temperature may transiently push the system towards an IMT, much like the structural phase transition in the metal oxide VO₂ ($T_c = 340$ K), where ultrafast light triggering of a nonthermal IMT has been well studied [6,13].

Ultrafast pump-probe techniques disentangle the complexity in such systems by identifying various relaxation channels in the time domain. In our earlier study [14], we used all-optical ultrafast reflectivity in the low-fluence regime to study the dynamics of the lattice and the $5f$ electrons. The measurements revealed a significant influence of the lattice deformation on the relaxation of photoexcited electrons and an unusually long, microsecond relaxation, especially below the Néel temperature ($T_N = 30$ K), attributed to the formation of polaronic excitons. Our experiments, contrary to expectations based on previous studies of oxide systems [6,13], show the

absence of a nonthermal IMT in UO₂ even at large pump fluences. The TRPES instrument that we use in this experiment was designed specifically to provide a probe photon energy at 32.55 eV sufficiently high for $5f$ photoionization cross sections to become significant [15] and pump energy at 3.1 and 4.65 eV comparable with the Mott gap. Successful results were obtained so far by utilizing this capability for time-resolved photoemission experiments in a number of complex electronic systems [3,16,17]. Details about the setup can be found in Ref. [15]. We used a hemispherical photoelectron spectrometer in angle-integrated mode, because the $5f$ LHB in UO₂ is only very weakly dispersive [7] in momentum space. Single crystal samples of [100] cubic UO₂ were cleaved *in situ* under ultrahigh vacuum ($< 10^{-10}$ Torr) to provide a fresh surface for pump-probe TRPES experiments. Finally, due to a rapid decrease in conductivity in UO₂ with decreasing sample temperature, low-temperature TRPES scans are impossible due to charging of the sample caused by the XUV beam.

An example static PES spectrum of UO₂ using our high-harmonic-generation-based XUV source is shown in the inset in Fig. 1(c). The PES spectrum of UO₂ is dominated by O $2p$ levels at less than -4 eV. The UO₂ LHB is characterized by the U $5f$ peak from -1 to -3 eV (below the Fermi level), consistent with previous synchrotron-based measurements [7]. The main plot in Fig. 1(c) shows the appearance of an excited state peak when pumping UO₂ at 4.65 eV with a fluence of 0.51, 0.39, 0.26, and 0.13 mJ/cm², respectively. The data in the plot are for conditions when the pump and probe pulses are overlapped in time (i.e., $t = 0$ time delay). The peak at 3 eV is ascribed to the UHB. We observe the Mott gap directly (see Fig. 1) and estimate it to be 2.5 eV, as measured between the midpoint of the LHB and UHB band edge slopes. Moreover, the high pump photon energy allows us to simultaneously map out the spectrum of the entire LHB and UHB, indicating that the on-site Coulomb interaction energy is about 5 eV as measured between the maximum intensities of both bands, respectively. Previously, this parameter has been accessed only indirectly via a combination of valence-band and inverse photoemission [10–12]. The net effect of increasing pump photon fluence is increasing of the energy spread and center of the mass position of carriers in the UHB.

Figure 2(a) is a color surface plot of the normalized spectral photoemission intensity of the populated states in the UHB over a 4.65-eV-pump-XUV-probe time delay range of -0.2 to 24.0 ps. The data clearly show a decay over the time scale of picoseconds with decreasing energy spread (W_{UHB}) in the UHB due to band relaxation from an initial ($t = 0$) width of 2.3 eV to 1.7 eV after 20 ps [Fig. 2(b)]. W_{UHB} is defined as the FWHM of the measured spectral weight at a particular time delay, and the binding energy E_{UHB} is computed from the measured kinetic energy

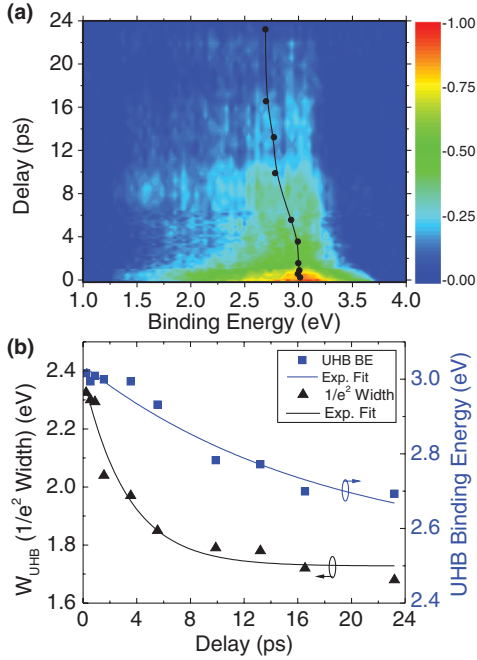


FIG. 2. Time-resolved band dynamics of UHB at 4.65-eV pump photon energy and fluence of 0.51 mJ/cm²: (a) surface plot of the TRPES spectrum of UHB as a function of pump-probe time delays up to $\Delta t = 24$ ps. The black line marks the binding energy (center of gravity) of UHB; (b) extracted UHB spectral width W_{UHB} and binding energy as the pump-probe delay is varied.

of the electrons by using the center of gravity energy position minus the Fermi energy. A corresponding shift in the position of E_{UHB} to lower energies is also observed. The change in E_{UHB} from 3.0 to 2.7 eV above E_F represents a shift of 15%. The UHB binding energy shift, however, does not appear to be purely a spectral weight redistribution of states of intraband type. Clear evidence of thermalization processes where high-lying states in the UHB relax to lower-lying levels is not observed. Instead, we observe a loss of spectral weight across the entire UHB with the most rapid (less than a picosecond at the highest excitation fluences) decay resulting from the highest populated states above 3.2 eV. Based on our previous ultrafast time-resolved optical reflectivity study [14], the observed UHB depopulation is too fast to be interpreted as direct recombination. Instead, we hypothesize that it may be spectral weight loss via indirect processes due to two possible mechanisms: (i) rapid loss at higher energies from phonon scattering due to larger scattering phase space volume; (ii) or more likely loss due to the UHB hybridizing with other bands (i.e., $6d$ levels of U, dispersive O $2p$ bands) that are known to exist at the high-energy tail end of the UHB [10]. This would open up the possibility of scattering into the portions of the 3D Brillouin zone that we are not probing. The data presented in Fig. 2(b) very clearly show that the width stabilizes around 1.7 eV at large delays, while binding

energy continues to shift down. This result is in contrast to TRPES studies of other Mott insulating systems such as 1T-TaS₂ [2], where upon photoexcitation a midgap band of renormalized electronic states is formed along with a rapid sub-300-fs decay of states above E_F . In the UO₂ case, the UHB appears as a robust spectral feature at all delays. The difference in these two cases is attributed to the large Coulomb interaction in UO₂ compared to $U_C \approx 0.6$ eV for 1T-TaS₂. Figure 2(a) shows that relaxation appears as spectral weight shifting towards the Mott gap. Extremely weak interband filling of spectral density between the LHB and UHB is observed without midgap quasiparticle peak generation, lending itself to interpretation that photodoping of carriers in this system leaves UO₂ in an excitonic Mott-Hubbard insulating state [18] without metallization or midgap band renormalization. Therefore, despite photodoping UO₂ with electron-hole pairs to fluences in the mJ/cm² range that correspond roughly to one $e-h$ pair excited per 100 U atomic sites, the increase in electronic energy is not sufficient to induce an IMT.

Also, we do not observe the well-defined exciton peaks, thought to be formed by the attractive holon-doublon interaction and expected to appear within the Mott gap. In contrast to typical band insulators, excitons in Mott-Hubbard insulators have been predicted to form either below or above the band edge, depending on the relative strengths of hopping, on-site, and nearest-neighbor interaction energies. [19]. This in fact has been observed experimentally in transition metal oxide Mott insulators such as YVO₃ [20]. Moreover, due to the anticipated broadening of the excitonic linewidth and the limitation of room temperature measurements, we were not able to directly observe excitonic peaks in the density of states.

Tuning the pump photon energy among the fundamental and harmonics allows us to impart various initial states with different kinetic energies. Results for pumping at 1.55 eV showed no TRPES signal generated from the time-delayed XUV probe pulse. This is consistent with a UO₂ Mott gap of $E_{\text{gap}} = 2.5$ eV and our earlier results from ultrafast time-resolved reflectivity studies [14]. In Fig. 3, we plot the energy-integrated spectral density as a function of the pump-probe time delay for each pump photon case: 3.1 and 4.65 eV, respectively. The colored line traces in each figure plot correspond to different pump fluences. The early time decay rates appear to display both fluence and pump photon energy dependence dominating the dynamics in the first 2 ps. The inset symbol plots in Fig. 3 are the TRPES relative signal amplitude versus fluence (at time delay $t = 0$). From the inset plots, TRPES amplitude signals at $t = 0$ display a fluence-dependent thresholdlike behavior that significantly alters the early time ($t \leq 2$ ps) amplitude and decay shapes. The similarity in the late time decay of the time-domain traces of Fig. 3 indicates a common recovery mechanism roughly independent of fluence and pump photon energy. The main traces in Fig. 3 are fitted to

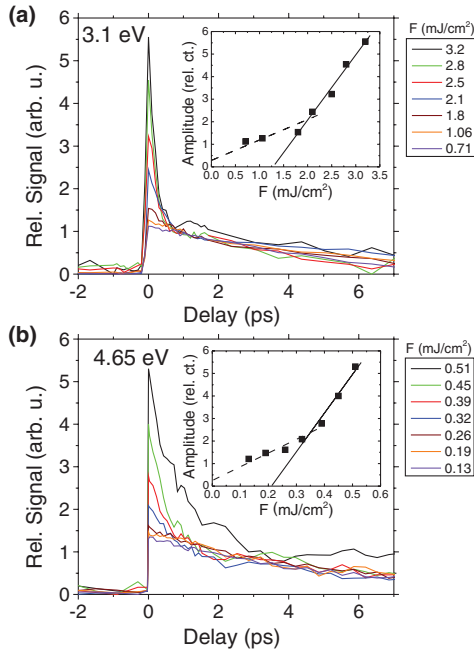


FIG. 3. Time-domain dynamics of the energy-integrated UHB spectral density for pump photon energies of (a) 3.1 and (b) 4.65 eV. The pump fluence is indicated by the different colored traces according to plot legend values. The inset plots show the fluence dependence of the signal amplitude at $t = 0$ time delay with a linear fit to the largest five fluences marking the fluence threshold ($F_{th} \approx 1.25$ mJ/cm² for 3.1 eV and $F_{th} \approx 0.22$ mJ/cm² for 4.65 eV) x intercept where higher-order interactions begin.

a two-term single exponential decay time model: $A \exp(-t/\tau_1) + B \exp(-t/\tau_2)$ with fast (τ_1) and slow (τ_2) time constants. The corresponding inverse decay constants are plotted as a function of fluence (F) in Fig. 4 for the 3.1- and 4.65-eV cases, respectively. In both pump photon energy cases, inverse τ_2 is approximately fluence independent, with a value of $\tau_2^{-1} \approx 0.125$ ps⁻¹ over a pump fluence range of $F = 0.71 - 3.2$ mJ/cm² for the 3.1-eV case [Fig. 4(a)] and $\tau_2^{-1} \approx 0.17$ ps⁻¹ over a pump fluence range of $F = 0.13 - 0.51$ mJ/cm² for the 4.65-eV case [Fig. 4(b)].

Turning our attention to the slow dynamics in Fig. 3, at longer time delay, we observe a time constant in the multipicosecond range. We can rule out electron-hole radiative recombination as the source of this reduction in signal, since this recombination has been shown to occur on the nanosecond time scale under ultrafast photoexcitation [14]. The presence of a nearly fluence-independent decay rate (τ_2^{-1}) is typically understood as a manifestation of a bottleneck effect. Here we ascribe this to a phonon bottleneck, where quasiequilibrium between the photoexcited carriers and the phonon bath is established. The observed “universal” decay with a time constant of $\approx 6-8$ ps then is characteristic of the time scale over which the transfer of energy from the electron to the phonon

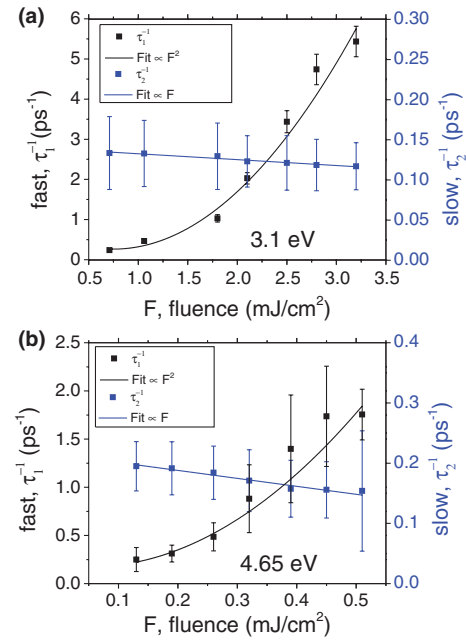


FIG. 4. Corresponding two-term exponential fit decay constants (fast, τ_1 ; slow, τ_2) to the data of Fig. 3 are plotted as a function of fluence for the (a) 3.1- and (b) 4.65-eV cases.

subsystems occurs and hints towards the formation of stable excitonic polarons consistent with the picosecond lattice deformation time observed by An *et al.* [14]. The fluence-independent dynamics suggests that the electron relaxation is mediated not by thermal phonons but by generation of hot optical phonons. Thus the loss of spectral weight at this time scale is ascribed to indirect electron-hole recombination accompanied possibly with multiphonon emission. In support of this scenario, strong electron-phonon interaction is known to be present in UO₂ forming small polarons through the electron and longitudinal optical phonon lattice interactions from defect states in the material [9]. After excitonic polarons are formed, subsequent recombination of carriers is governed by the decay of the phonon modes most strongly coupled to the electrons. As this phonon cooling can be a very slow process, it is expected that corresponding quasiparticles can exhibit very long lifetimes, especially at low temperatures [14]. As our experimental setup is most sensitive to large changes occurring on a relatively short time scale, we do not observe this long-lived dynamics, but our earlier high-sensitivity measurements have indeed indicated long, nanosecond recombination dynamics at room temperature.

The fast subpicosecond dynamics contained in the τ_1^{-1} data plotted in Fig. 4, however, show a pronounced fluence dependence. This part of the UHB population dynamics appears to be dominated by the threshold fluence dependence (see the inset in Fig. 3) of the signal at $t = 0$. Surprisingly, the integrated spectral intensity is reduced to a fluence independent value within ~ 1 ps. From Fig. 1(c), we observe that increasing fluence spreads the

accessed states over a wider energy distribution in the UHB, and the integrated time-domain dynamics shown in Fig. 3(a) show a strong increase in spectral weight that then rapidly decays. The threshold fluences of 1.25 and 0.22 mJ/cm² determined from Fig. 3 at 3.1- and 4.65-eV excitation energies, respectively, correspond to an absorbed fluence threshold F_{th} , of 0.02 eV per U atom taking into account optical absorption at 3.1 (0.007 nm⁻¹) and 4.65 eV (0.01 nm⁻¹) photon energies [21]. The nonlinear fluence dependence of τ_1 for the 3.1- and 4.65-eV cases suggests that high-order processes begin to dominate in this regime. At F_{th} the electron distribution is driven strongly out of equilibrium, and the shape of the UHB is distorted with significant electron spectral density appearing at the high-energy side. On this very short time scale, dictated by strong electron-electron interactions, this could lead to electrons transiently populating states lying much higher than suggested by the pump photon energy [17]. This is evidenced by the fact that such a highly nonthermal state could be reached at both excitation photon energies (3.1 and 4.65 eV) and is therefore a consequence of the density of photoexcited electrons. Having reached these high-energy states, the electrons have a large phase space available for scattering as previously discussed: efficient interaction with strongly coupled phonon modes allows for rapid cooling in the first 2 ps with interband scattering to more dispersive U 6*d* and O 2*p* bands until a quasiequilibrium state with the lattice is reached. Therefore, the fast dynamics are indicative of the density-dependent relaxation of electrons residing in the high-energy states in the UHB through these processes.

Our study provides the first direct, single-experiment measurement of the Hubbard gap in a 5*f* Mott insulator. In conclusion, despite significant photodoping, we do not observe an IMT but rather a robust Mott gap structure attributed to the strong on-site Coulomb interaction. We conclude that, with no exciton bands observed, the universal slow relaxation time τ_2 and the nonlinear response of τ_1 indicate that pair collisions of polaronic Hubbard excitons dominate the long time response, and their lifetime is mediated by interaction with phonons. This finding opens the possibility for future investigations of the quasiparticle physics on the ultrafast scale using 5*f*-electron Mott systems as an accessible test bed for exotic behavior of doubly occupied states in the limit of large U_C .

Funding for this work was provided by the Laboratory Directed Research and Development and by the Basic Energy Sciences programs at Los Alamos National Laboratory under the auspices of the Department of Energy for Los Alamos National Security LLC under Contract No. DEAC52-06NA25396 and by Office of Basic Energy Sciences, Division of Material Sciences.

*rodrigeo@lanl.gov

- [1] S. Wall, D. Brida, S. R. Clark, H. P. Ehrke, D. Jaksch, A. Ardavan, S. Bonora, H. Uemura, Y. Takahashi, T. Hasegawa, H. Okamoto, G. Cerullo, and A. Cavalleri, *Nat. Phys.* **7**, 114 (2010).
- [2] L. Perfetti, P. A. Loukakos, M. Lisowski, U. Bovensiepen, M. Wolf, H. Berger, S. Bierman, and A. Georges, *New J. Phys.* **10**, 053019 (2008).
- [3] J. C. Petersen, S. Kaiser, N. Dean, A. Simoncig, H. Y. Liu, A. L. Cavalieri, C. Cacho, I. C. E. Turcu, E. Springate, F. Frassetto, L. Poletto, S. S. Dhesi, H. Berger, and A. Cavalleri, *Phys. Rev. Lett.* **107**, 177402 (2011).
- [4] K. A. Al-Hassanieh, F. A. Reboredo, A. E. Feiguin, I. González, and E. Dagotto, *Phys. Rev. Lett.* **100**, 166403 (2008).
- [5] S. Y. Yang, J. Seidel, S. J. Byrnes, P. Shafer, C.-H. Yang, M. D. Rousell, P. Yu, Y.-H. Chu, J. F. Scott, J. W. Ager, III, L. W. Martin, and T. Ramesh, *Nat. Nanotechnol.* **5**, 143 (2010).
- [6] C. Kübler, H. Ehrke, R. Huber, R. Lopez, A. Halabica, R. F. Haglund, Jr., and A. Leitenstorfer, *Phys. Rev. Lett.* **99**, 116401 (2007).
- [7] L. E. Roy, T. Durakiewicz, R. L. Martin, J. E. Peralta, G. E. Scuseria, C. G. Olson, J. J. Joyce, and E. Guzewicz, *J. Comput. Chem.* **29**, 2288 (2008).
- [8] M. Eckstein and P. Werner, *Phys. Rev. Lett.* **110**, 126401 (2013).
- [9] P. Ruello, K. D. Becker, K. Ullrich, L. Desgranges, C. Petot, and G. Petot-Ervas, *J. Nucl. Mater.* **328**, 46 (2004).
- [10] J. G. Tobin and S.-W. Yu, *Phys. Rev. Lett.* **107**, 167406 (2011).
- [11] P. Roussel, P. Morrall, and S. J. Hull, *J. Nucl. Mater.* **385**, 53 (2009).
- [12] S.-W. Yu, J. G. Tobin, J. C. Crowhurst, S. Sharma, J. K. Dewhurst, P. Olalde-Velasco, W. L. Yang, and W. J. Siekhaus, *Phys. Rev. B* **83**, 165102 (2011).
- [13] A. Cavalleri, Cs. Tóth, C. W. Siders, J. A. Squier, F. Ráksi, P. Forget, and J. C. Kieffer, *Phys. Rev. Lett.* **87**, 237401 (2001).
- [14] Y. Q. An, A. J. Taylor, S. D. Conradson, S. A. Trugman, T. Durakiewicz, and G. Rodriguez, *Phys. Rev. Lett.* **106**, 207402 (2011).
- [15] G. L. Dakovski, Y. Li, T. Durakiewicz, and G. Rodriguez, *Rev. Sci. Instrum.* **81**, 073108 (2010).
- [16] G. L. Dakovski, Y. Li, S. M. Gilbertson, G. Rodriguez, A. V. Balatsky, J.-X. Zhu, K. Gofryk, E. D. Bauer, P. H. Tobash, A. Taylor, J. L. Sarrao, P. M. Oppeneer, P. S. Riseborough, J. A. Mydosh, and T. Durakiewicz, *Phys. Rev. B* **84**, 161103 (R) (2011).
- [17] S. Gilbertson, G. L. Dakovski, T. Durakiewicz, J.-X. Zhu, K. M. Dani, A. D. Mohite, A. Dattelbaum, and G. Rodriguez, *J. Phys. Chem. Lett.* **3**, 64 (2012).
- [18] Y. Tomio and T. Ogawa, *J. Phys. Soc. Jpn.* **79**, 104707 (2010).
- [19] F. H. L. Essler, F. Gebhard, and E. Jeckelmann, *Phys. Rev. B* **64**, 125119 (2001).
- [20] F. Novelli, D. Fausti, J. Reul, F. Cilento, P. H. M. van Loosdrecht, A. A. Nugroho, T. T. M. Palstra, M. Grüninger, and F. Parmigiani, *Phys. Rev. B* **86**, 165135 (2012).
- [21] T. T. Meek, B. von Roedern, P. G. Clem, and R. J. Hanrahan, Jr., *Mater. Lett.* **59**, 1085 (2005).